

UDC 621.373.122

## ANALYSIS OF SIGNALS OF STABILIZED AUTODYNES

Vladislav Ya. Noskov<sup>1</sup>, Kirill A. Ignatkov<sup>1</sup>, Sergey M. Smolskiy<sup>2</sup><sup>1</sup>Ural Federal University (UPI), Ekaterinburg, Russia<sup>2</sup>Moscow Power Engineering Institute (Technical University), Moscow, Russia

Results of the autodyne signal analysis of the self-oscillating systems stabilized in frequency by the external high-quality cavity are given. The coupling between the main and stabilizing cavities is realized on the basis of a pass-reflective filter with a resistive link. Mathematical equations are obtained describing an autodyne response onto impact of the own radiated signal reflected from a target. The analysis of phase, amplitude, frequency and amplitude-frequency characteristics of the autodyne system is fulfilled. The calculation of an autodyne signal spectrum is discussed. A new type of nonlinear distortions of an autodyne signal is examined, which is caused by a frequency dispersion of an oscillating system of the stabilized autodyne. Advantages of the stabilized autodyne compared to the usual single-tuned autodyne oscillator are shown.

### Introduction

Autodyne oscillators (or simply autodynes) are widely used in the compact short-range radar systems, in measuring equipment for aeroballistic testing, in guard devices, in sensors and measuring systems of different parameters on transport, in industry and in scientific researches [1–7]. A combination of functions of the probing electromagnetic radiation transmitter and receiver of the reflected signal from a target in the single oscillator (autodyne) provides the constructive simplicity, compactness and the relatively low cost of an UHF module of the autodyne short-range radar.

The principle of these devices operation is based on the phenomenon of oscillations amplitude and frequency variations as well as an average value of current or voltage variations in the supply circuit of an active element (AE) at the influence of the own reflected radiation. By means of the devices for autodyne response extraction these variations are converted into the output signal (current or voltage), which is suitable for the further processing. These signals processing provides the information about the reflecting objects and the parameters of their movement.

Autodyne transmitter-receiver (or transceiver) devices are permanently improved and its application areas are widened [7–9]. Development of autodyne systems is going on the way of assimilation of a millimeter wavelength range and creation of the hybrid-integrated modules [2, 8, 9]. At this wavelength range assimilation there are a number of problems, one of which is linked with appearance of the signal nonlinear distortions at the increase of level and delay time of reflected radiation [10–13]. These distortions caused by the autodyne frequency variations are unwanted at many autodyne

applications since they create the serious problems at signal processing, especially in the case of the spatially distributed reflecting objects [14].

To reduce the signal distortion level and the influence of various destabilizing environment factors (among which the temperature is the key factor) upon the technical characteristics of autodyne systems, in [12–14] it was offered to stabilize the frequency of the autodyne oscillator by the external high-quality cavity (resonator). At the investigation of such autodyne, it is necessary to use the double-tuned model of the oscillating system.

Double-tuned and more complicated triple-tuned models were investigated in publications [7, 15, 16], which were devoted to autodyne examination used in UHF radio spectroscopy as well as in techniques for inspection of the material parameters and articles dimensions. In [17] the research of biharmonic autodynes is offered, which use the additional cavity at the second harmonic for the frequency stabilization.

Nevertheless, in known publications devoted to the radar applications of the single-frequency autodynes containing the basic and additional stabilizing cavities, the output signal analysis is absent, although the results of these investigations are undoubtedly interesting to determine the potential opportunities of such autodynes and to widen its application area.

The aim of this paper is to conduct the analysis of autodyne signals of the self-oscillating system in the form of combination of the main and stabilizing cavities, the theoretical investigation of phase, amplitude, frequency, amplitude-frequency and spectral characteristics of the autodyne system, as well as formation of recommendations on development of autodyne short-range radar for various purposes.

### Equivalent circuit of stabilized autodyne oscillator

For mathematical description of the principal aspects in the system under analysis, we consider the functional scheme of the simple autodyne radar presented in Fig. 1a, in which the autodyne oscillator (AO), stabilized by the external cavity (EC), is implemented on the basis of one-port AE of  $N$ - or  $S$ -type (Gunn diode, IMPATT diode). The oscillator AO is directly connected with the transmitting-receiving antenna A, through which its interaction with returned radiation from the reflecting object (RO) (or reflector) takes place.

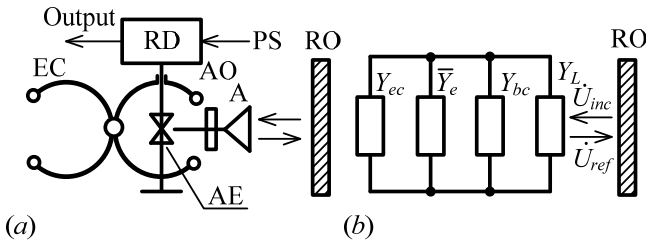


Fig. 1. The functional (a) and equivalent (b) schemes of the stabilized autodyne oscillator.

At that, autodyne variations of the average value of current or voltage in the AE supply circuit arising are converted into the voltage of the “output” auto-detecting signal by means of the registration device RD [18]. In some constructions of autodyne short-range radar the useful signal is extracted by an external detector, which converts the autodyne variations of oscillation amplitude or frequency into the output signal voltage [14].

An equivalent circuit of the autodyne oscillator reduced to the AE plane is presented in Fig. 1b. In this high-frequency circuit the stabilizing cavity (external cavity) and the basic (operating) cavity are presented by conductivities  $Y_{ec}$  and  $Y_{bc}$ , accordingly, and  $Y_L$  represents the conductivity of an oscillator load and its variations caused by an impact of reflected radiation. The average (over the oscillation period) electronic conductivity of AE  $\bar{Y}_e$  in the general case depends on the bias voltage  $E$ , the amplitude  $A$  and frequency  $\omega$  of oscillations:  $\bar{Y}_e = \bar{Y}_e(E, A, \omega)$ . In accordance with the general theory of UHF oscillators [19], the oscillation equation for the equivalent circuit shown in the Fig. 1b takes the form:

$$Y_\Sigma = G_\Sigma + jB_\Sigma = Y_{ec} + \bar{Y}_e + Y_{bc} + Y_L = 0. \quad (1)$$

The reflected wave action in equation (1), according to the equivalent circuit method known in practice of UHF circuit calculation, is presented by the variable load  $Y_L$  [11, 19, 20]. Assume that the incident wave in

the form of sinusoidal voltage and current for the given time moment  $t$  is specified by expressions  $\dot{U}_{inc}(t) = U_{inc}(t)\exp\Psi_u(t)$  and  $\dot{I}_{inc}(t) = I_{inc}(t)\exp\Psi_i(t)$ . Then the reflected wave, which energy was created by the oscillator at time moment  $t - \tau$ , can be presented in the form of voltage  $\dot{U}_{ref}(t, \tau) = U_{ref}(t, \tau)\exp\Psi_u(t, \tau)$  and current  $\dot{I}_{ref}(t, \tau) = I_{ref}(t, \tau)\exp\Psi_i(t, \tau)$ . Here  $\tau = 2s/c$  is the time of radiation propagation to the reflecting object and back;  $s$  is the distance to the reflector;  $c$  is the velocity of radiation propagation. Using these expressions we obtain the equation for the complex voltage reflection factor  $\dot{\Gamma}(t, \tau)$  from the load  $Y_L$ :

$$\begin{aligned} \dot{\Gamma}(t, \tau) &= \frac{\dot{U}_{ref}(t, \tau)}{\dot{U}_{inc}(t)} = \Gamma \frac{U_{ref}(t, \tau)}{U_{inc}(t)} \exp[-\delta(t, \tau)] = \\ &= \Gamma \sqrt{\frac{P_{ref}(t, \tau)}{P_{inc}(t)}} \exp[-\delta(t, \tau)] = \Gamma(t, \tau) \exp[-\delta(t, \tau)], \quad (2) \end{aligned}$$

where  $P_{inc}(t)$ ,  $P_{ref}(t, \tau)$  are powers of radiated signals on the oscillator load at time moments  $t$  and  $(t - \tau)$ , respectively;  $\Gamma(t, \tau)$  and  $\delta(t, \tau)$  are the instantaneous values of modulus and phase of the reflection factor. At that,  $\Gamma$  characterizes the radiation damping at its propagation to the object and back, and  $\delta(t, \tau) = \Psi_u(t) - \Psi_u(t, \tau)$  is the complete phase incursion of the reflected wave.

Taking (2) into consideration, we obtain the expression for the conductivity  $Y_L$ :

$$Y_L(t, \tau) = \frac{\dot{I}_L(t, \tau)}{\dot{U}_L(t, \tau)} = G_L \frac{1 - \dot{\Gamma}(t, \tau)}{1 + \dot{\Gamma}(t, \tau)}, \quad (3)$$

where  $G_L$  is the conductivity of the oscillator load at absence of the reflected wave, when  $\Gamma(t, \tau) = 0$ . Equations (2) and (3), in contrast to known equations [11, 19, 20], take into account the impact of the own reflected radiation as a result of amplitude-phase lag on time  $\tau$  of oscillations influencing from the previous state of a system. The correct account of this phenomenon seems to us important enough at analysis of radar applications of autodynes, especially with using various types of modulation [21–24].

Since in real conditions of autodyne system functioning, the amplitude of natural oscillations considerably exceeds the amplitude of signals returned from the reflector to the main cavity, so the condition  $\Gamma \ll 1$  is fulfilled and equation (3) can be simplified:

$$\begin{aligned} Y_L(t, \tau) &= G_L - 2G_L\Gamma(t, \tau)\cos\delta(t, \tau) + \\ &+ j2G_L\Gamma(t, \tau)\sin\delta(t, \tau) = G_L + \Delta Y_L(t, \tau), \quad (4) \end{aligned}$$

where  $\Delta Y_L(t, \tau) = -\Delta G_L(t, \tau) + j\Delta B_L(t, \tau)$  is the complex conductivity caused by the action of the reflected wave;

$\Delta G_L(t, \tau) = 2G_L \Gamma(t, \tau) \cos \delta(t, \tau)$  and  $\Delta B_L(t, \tau) = j2G_L \times \Gamma(t, \tau) \sin \delta(t, \tau)$  are its resistive and reactive components.

From the practice of frequency stabilization of UHF oscillators by external high- $Q$  cavities, the resistive method of stabilizing cavity connection is known [25, 26], which has an advantage of unambiguity of tuning characteristics in the operating frequency range. This property of the oscillating system is necessary for obtaining the high-quality autodyne signal with absence of step-wise variations of oscillation parameters in the wide range of input signal amplitudes. The simplest way of constructive realization of this coupling is connection of the external cavity in the form of pass-band reflective filter.

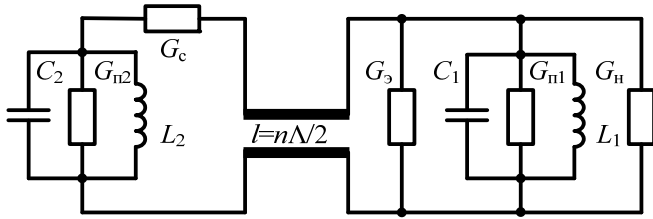


Fig. 2. The equivalent circuit of the oscillating system with resistive coupling between cavities.

The equivalent circuit of such oscillation system is shown in Fig. 2. Here  $\bar{G}_e$  is the active conductance of AE connected in parallel to the first tank. This tank including passive components of AE as well as the inductance  $L_1$ , the capacitance  $C_1$  and the conductance of inherent losses  $G_{r1}$ , represents the equivalent of the basic oscillator cavity. The second (stabilizing) cavity is also presented in Fig. 2 by the parallel tank, which contains the inductance  $L_2$ , the capacitance  $C_2$  and the conductance of inherent losses  $G_{r2}$ . The transmission line segment between cavities matched with the resistive coupling conductance  $G_c$  has the length  $l$ , which is multiple of half wavelength in the waveguide:  $l = n\lambda/2$ , where  $n = 1, 2, \dots$ .

The conductance of the considered oscillating system reduced to connection terminal of AE at the oscillation frequency  $\omega_0$  without the reflected radiation, when  $\Gamma = 0$ , is defined by the following equation [27]:

$$\begin{aligned}
 Y_{os} &= G_{os} + jB_{os} = Y_{er} + Y_{bc} + G_L = \\
 &= G_1 \left[ 1 + \frac{\beta_1(1 + j2Q_{c2}v_{c2})}{(1 + \beta_2) + j2Q_{c2}v_{c2}} + j2Q_{L1}v_{c1} \right], \quad (5)
 \end{aligned}$$

where  $\beta_1 = G_c/G_1$ ,  $\beta_2 = G_c/G_{r2}$  are coefficients characterizing the coupling degree of the based and stabilizing cavities with the transmission line;  $v_{c1} = (\omega - \omega_0)/\omega_{c1}$ ,  $v_{c2} = (\omega - \omega_{c2})/\omega_{c2}$  are relative offsets of current fre-

quencies of the first  $v_{c1}$  and the second (stabilizing)  $v_{c2}$  cavities, having the natural frequencies  $\omega_{c1} = 1/(L_1C_1)^{1/2}$ ,  $\omega_{c2} = 1/(L_2C_2)^{1/2}$  and  $Q$ -factors of the first (loaded)  $Q_{L1} = \omega_{c1}C_1/G_1$  and the second (unloaded)  $Q_{c2} = \omega_{c2}C_2/G_{r2}$  cavities;  $G_1 = G_{r1} + G_L$ .

Separating the real and imaginary parts in (5) and performing its normalization with respect to the value  $G_1$ , we obtain:

$$g_{os}(v_{c2}) = \frac{G_{os}}{G_1} = 1 + \beta_1 \frac{1 + \beta_2 + 4Q_{c2}^2v_{c2}^2}{(1 + \beta_2)^2 + 4Q_{c2}^2v_{c2}^2}; \quad (6)$$

$$b_{os}(v_{c2}) = \frac{B_{os}}{2G_1} = Q_{L1}v_{c1} + \frac{\beta_1\beta_2Q_{c2}v_{c2}}{(1 + \beta_2)^2 + 4Q_{c2}^2v_{c2}^2}. \quad (7)$$

Graphs of frequency dependences of the normalized conductances  $g_{os}(v_{c2})$  and  $b_{os}(v_{c2})$  calculated according to (6) and (7) for  $Q$ -factor  $Q_{c2} = 1000$  are presented in Fig. 3. In the calculation we took into consideration the matching condition of the connecting line with the stabilizing cavity, at which  $\beta_2 = 1$  and the fixing capability of the stabilizing cavity is maximal, for different values of the  $\beta_1$  parameter, defining the coupling degree with the basic cavity.

It should be noted that characteristics obtained at  $\beta_1 = 0$  (curves 4) correspond to the autodyne with the single-tank oscillating system.

As follows from Fig. 3a, the frequency characteristic of the reactive  $b_{os}(v_{c2})$  component of oscillation system conductivity under condition of exact tuning of the stabilizing cavity, when  $v_{c2} = 0$ , has the central symmetry whereas the same characteristics of the resistive  $g_{os}(v_{c2})$  component have the axis symmetry. At that, if the coupling parameter  $\beta_1$  between cavities is less than its critical value  $\beta_{cc}$ , which in this case equals to  $\beta_{cc} = 3.4$ , then characteristics  $b_{os}(v_{c2})$  are unambiguous frequency functions (curves 2, 3). If this inequality is not fulfilled, deflections appear (curve 1). Parts of these characteristics, where its derivatives have the negative sign, are unstable [25].

In the case  $\beta_1 \leq \beta_{cc}$ , the operation point on characteristics  $b_{os}(v_{c2})$  moves steadily due to autodyne frequency variations, without trajectory jumps. Whereas at this inequality fulfillment another qualitatively situation is observed in the operation point movement. In this case the point on these characteristics passes during movement through unstable parts with the negative derivative by the jumps with hysteresis phenomena. At another  $Q$ -factor  $Q_{c2}$  the magnitude of critical coupling  $\beta_1 = \beta_{cc}$  has another value. This value of the coupling parameter  $\beta_{cc}$  indicates the boundary between the cases of strong ( $\beta_1 > \beta_{cc}$ ) and weak ( $\beta_1 < \beta_{cc}$ ) coupling be-

tween cavities, since it defines qualitative differences in the character of autodyne frequency variations.

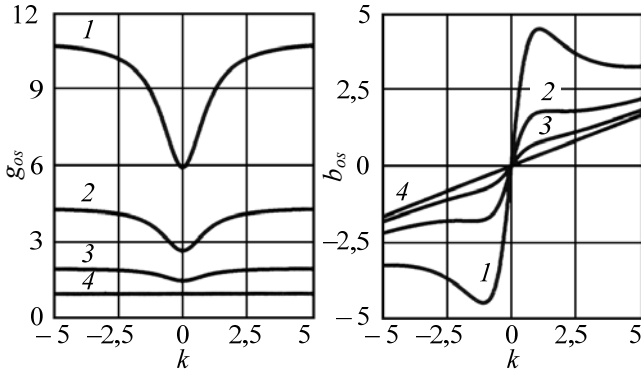


Fig. 3. Normalized curves of resistive  $g_{os}$  and reactive  $b_{os}$  conductance of the oscillating system depending on the generalized offset  $v_{c2}$ , calculated for  $Q_{L1} = 100$ ,  $Q_{c2} = 1000$ ,  $\beta_2 = 1$ ,  $k = v_{c2} \cdot 10^{-3}$  and the following coupling parameters: (1)  $\beta_1 = 10$ ; (2)  $\beta_1 = 3.4$ ; (3)  $\beta_1 = 1$ ; (4)  $\beta_1 = 0$ .

Comparison of curves 1–3 and the curve 4 shows that in double-tank oscillating system the frequency function character essentially differs from the similar characteristics of the usual single-tank oscillator. The presence of sharp dip in  $g_{os}(v_{c2})$  limits the amplitude balance in the frequency band and improves excitation conditions of the single-frequency oscillations. The slope of the linear part in the center of the function  $b_{os}(v_{c2})$ , caused by the stabilizing cavity action is equal to the equivalent  $Q$ -factor  $Q_{equ}$  of the considered oscillating system:

$$Q_{equ} = \omega_0 \left( \frac{db_{os}(v_{c2})}{d\omega} \right)_0 = Q_{L1} + \frac{\beta_1 \beta_2}{(1 + \beta_2)^2} Q_{c2}.$$

This  $Q$ -factor characterizing the fixing capability in frequency for the stabilizing oscillator is usually much higher than for single-tank oscillator having the  $Q$ -factor  $Q_{L1}$ . Mentioned features of characteristics  $g_{os}(v_{c2})$  and  $b_{os}(v_{c2})$  of the considered oscillating system will be taken into account in the further analysis of processes in the stabilized autodyne oscillator.

### Key relations for analysis of stabilized autodyne

From condition of self-oscillations (1) taking into account (4), (6) and (7), we obtain equations for the quasi-static analysis of the autodyne oscillator:

$$G_{\Sigma} = \bar{G}_e + G_{os} - 2G_1 \Gamma(t, \tau) \eta \cos \delta(t, \tau) = 0; \quad (8)$$

$$B_{\Sigma} = \bar{B}_e + B_{os} + 2G_1 \Gamma(t, \tau) \eta \sin \delta(t, \tau) = 0, \quad (9)$$

where  $\eta = G_L / G_1 = Q_{L1} / Q_{ex1}$  is the efficiency of the based cavity;  $Q_{ex1} = \omega_{c1} C_1 / G_{L1}$  is its external  $Q$ -factor;

$$G_{os} = G_1 + \frac{G_1 \beta_1 (1 + \beta_2 + 4Q_{c2}^2 v_{c2}^2)}{(1 + \beta_2)^2 + 4Q_{c2}^2 v_{c2}^2}, \quad (10)$$

$$B_{os} = 2G_1 Q_{L1} v_{c1} + \frac{2G_1 \beta_1 \beta_2 Q_{c2} v_{c2}}{(1 + \beta_2)^2 + 4Q_{c2}^2 v_{c2}^2} \quad (11)$$

are resistive and reactive components of the oscillating system conductivity, respectively.

Finding the solution of equations (8) and (9) represents the essential complexities because of the presence of nonlinear terms  $\bar{G}_e$  and  $\bar{B}_e$  depending on the bias voltage  $E$ , amplitude  $A$  and frequency  $\omega$  of oscillations. In order to find the approximate solution of the equation system (8), (9), we assume that variations of the stationary oscillation mode caused by the reflected radiation impact are sufficiently small. Then, the further analysis can be fulfilled in linear approximation for small variations of self-oscillation parameters in the vicinity of the steady-state mode.

At first, we find the parameters of the steady-state oscillation mode from the equation system (8), (9) at  $\Gamma(t, \tau) = 0$  assuming that  $E = E_0$ ,  $A = A_0$ ,  $\omega = \omega_0$ , and also  $\bar{G}_e = \bar{G}_{e0}$ ,  $\bar{B}_e = \bar{B}_{e0}$  and the average value of AE current  $\bar{I}_e = \bar{I}_{e0}$ . Then the operation mode of the non-disturbed autonomous double-tank oscillator is described by equations:

$$\begin{aligned} \bar{G}_{e0} + G_{os0} &= 0; \quad \bar{B}_{e0} + B_{os0} = 0; \\ \bar{I}_{e0} &= \bar{I}_{e0}(E_0, A_0, \omega_0), \end{aligned} \quad (12)$$

where  $\bar{G}_{e0} = \bar{G}_{e0}(E_0, A_0, \omega_0)$ ;  $\bar{B}_{e0} = \bar{B}_{e0}(E_0, A_0, \omega_0)$ ;  $G_{os0} = G_1 + \bar{G}_{20}$  is the oscillating system conductance, consisting of the loaded conductance  $G_1$  of the based cavity and the insertion conductance  $\bar{G}_{20} = G_1 \beta_1 / (1 + \beta_2)$  of the stabilizing cavity;  $B_{os0} = 2G_1 Q_{L1} v_{01}$  is the reactive component of the oscillating system conductance;  $v_{01} = (\omega_0 - \omega_{c1}) / \omega_{c1}$  is the relative offset of the based cavity frequency  $\omega_{c1}$  and the steady-state oscillation frequency  $\omega_0$  of an autonomous oscillator. This frequency can be calculated using (12):

$$\omega_0 = \omega_{c1} (1 + \tan \Theta / 2Q_{L1}), \quad (13)$$

where  $\Theta = \arctan(\bar{B}_{e0} / \bar{G}_{e0})$  is the phase shift inserted by AE. Expressions (12), (13) represent the steady-state equations, which are well known in the nonlinear oscillation theory for determination of amplitude and frequency of the autonomous single-tank oscillator [19].

Now, let us obtain equations in variations for the autodyne response of the double-tank oscillator relative to steady-state mode using equations (8)–(11) with account of (12) and (13). For this, we present the AE bias voltage, oscillation amplitude and frequency in the

form:  $E = E_0 + \Delta E$ ;  $A = A_0 + \Delta A$ ;  $\omega = \omega_0 + \Delta\omega$ , where  $\Delta E$ ,  $\Delta A$ ,  $\Delta\omega$  are the appropriate variations of steady-state parameters. At that, parameters  $\bar{I}_e$ ,  $\bar{G}_e$  and  $\bar{B}_e$ , being included in equations (8), (9), will get the appropriate variations in the vicinity of its steady-state values (12). We also take into consideration variations of autodyne response in an auto-detecting process. As a result, due to autodyne variations of the average value of the AE current  $\bar{I}_e = \bar{I}_e(E, A, \omega)$ , the possibility of the output autodyne signal extraction occurs in the oscillator supply circuit. Assuming that the variations of bias and oscillation are small enough, so that conditions of  $E_0 \gg \Delta E$ ,  $A_0 \gg \Delta A$ ,  $\omega_0 \gg \Delta\omega$  are fulfilled, the mentioned parameters can be presented in the following form with account of the first two expansion terms in Taylor series:

$$\bar{G}_e = G_{e0} + \left( \frac{\partial \bar{G}_e}{\partial E} \right)_0 \Delta E + \left( \frac{\partial \bar{G}_e}{\partial A} \right)_0 \Delta A + \left( \frac{\partial \bar{G}_e}{\partial \omega} \right)_0 \Delta \omega, \quad (14)$$

$$\bar{B}_e = B_{e0} + \left( \frac{\partial \bar{B}_e}{\partial E} \right)_0 \Delta E + \left( \frac{\partial \bar{B}_e}{\partial A} \right)_0 \Delta A + \left( \frac{\partial \bar{B}_e}{\partial \omega} \right)_0 \Delta \omega, \quad (15)$$

$$\bar{I}_e = I_{e0} + \left( \frac{\partial \bar{I}_e}{\partial E} \right)_0 \Delta E + \left( \frac{\partial \bar{I}_e}{\partial A} \right)_0 \Delta A + \left( \frac{\partial \bar{I}_e}{\partial \omega} \right)_0 \Delta \omega. \quad (16)$$

Hereinafter, the index “0” in partial derivatives means that their values are obtained in the vicinity of the steady-state mode.

The oscillating system of the oscillator under investigation differs by considerable conductance non-uniformity in the vicinity of the steady-state mode. At that, the resistive  $G_{os}$  and reactive  $B_{os}$  components are an even and odd functions of frequency, respectively. Therefore, when expanding these conductances into Taylor series, it is enough to take into account the first and third series terms in the resistive component and the first two series terms in the reactive component. Taking this into consideration, we obtain:

$$\begin{aligned} G_{os} &= G_{os0} + (1/2)(\partial^2 G_{os}/\partial \omega^2)_0 \Delta \omega^2, \\ B_{os} &= B_{os0} + (\partial B_{os}/\partial \omega)_0 \Delta \omega, \end{aligned} \quad (17)$$

where  $(\partial^2 G_{os}/\partial \omega^2)_0 = 8G_1[\beta_1\beta_2/(1+\beta_2)^3](Q_{c2}/\omega_{c2})^2$ ;  $(\partial B_{os}/\partial \omega)_0 = 2G_1[(Q_{L1}/\omega_{c1}) + (Q_{c2}/\omega_{c2})\beta_1\beta_2/(1+\beta_2)^2]$ .

Substituting (14)–(17) into (8), (9) and taking into account (12), we obtain the system of linearized equations for determination of the relative variations of amplitude  $a_1 = \Delta A/A_0$  and frequency  $\chi = \Delta\omega/\omega_0$ , as well as the current  $i_0 = \Delta \bar{I}_e/I_{e0}$  and the AE bias voltage  $a_0 = \Delta E/E_0$

$$\alpha_{10}a_0 + \alpha_{11}a_1 + \varepsilon_1\chi + \varepsilon_{n2}\chi^2 = \Gamma(t, \tau)\eta \cos \delta(t, \tau); \quad (18)$$

$$\beta_{01}a_0 + \beta_{11}a_1 + \xi\chi = -\Gamma(t, \tau)\eta \sin \delta(t, \tau); \quad (19)$$

$$\alpha_{00}a_0 + \alpha_{01}a_1 + \varepsilon_0\chi = i_0, \quad (20)$$

where  $\alpha_{00} = (E_0/\bar{I}_{e0})(\partial \bar{I}_e/\partial E)$  is the normalized differential conductance of AE in its supply circuit in the oscillation mode;  $\alpha_{01} = (A_0/\bar{I}_{e0})(\partial \bar{I}_e/\partial A)$  is the dimensionless parameter describing the phenomenon of auto-detecting of the oscillation amplitude;  $\varepsilon_0 = (\omega_0/\bar{I}_{e0}) \times (\partial \bar{I}_e/\partial \omega)$  is the parameter defining the contribution of frequency variations into variations of AE supply current (frequency auto-detecting);  $\alpha_{10} = (E_0/2\bar{G}_{e0}) \times (\partial \bar{G}_e/\partial E)$  is the parameter taking into account the amplitude modulation at variation of the bias voltage;  $\alpha_{11} = (A_0/2\bar{G}_{e0})(\partial \bar{G}_e/\partial A)$  is the reduced slope of the oscillator increment defining the regeneration degree and the strength of its limit cycle;  $\varepsilon_1 = (\omega_0/2\bar{G}_{e0}) \times (\partial \bar{G}_e/\partial \omega)$  is the influence factor of frequency variations onto the oscillation amplitude;  $\varepsilon_{n2} = 4Q_{c2}^2\beta_1 \times \beta_2/(1+\beta_2)^3$  is the parameter taking into account the nonlinear character of the autodyne response  $a_1$  due to the frequency function  $G_{os}$ ;  $\beta_{10} = (E_0/2\bar{B}_{e0})(\partial \bar{B}_e/\partial E) \times \tan\Theta$  is the parameter of the modulation sensitivity of the oscillator frequency to small variations of the bias voltage;  $\beta_{11} = (A_0/2\bar{B}_{e0})(\partial \bar{B}_e/\partial A)\tan\Theta$  is the parameter of oscillator’s anisochronous property;  $\xi = \xi_e + \xi_1 + \xi_2$ ;  $\xi_e = -(\omega_0/2\bar{B}_{e0})(\partial \bar{B}_e/\partial \omega)\tan\Theta$  is the parameter considering the frequency slope of the AE reactive conductance;  $\xi_1 = Q_{L1}$ ,  $\xi_2 = Q_{c2}[\beta_1\beta_2/(1+\beta_2)^2]$  are parameters of the frequency slope of the reactive conductance of based and stabilizing cavities. For the specific implementation of the oscillator these parameters can be calculated or determined experimentally.

Equations (18)–(20) describe the steady-state values and quasi-static variations of the self-oscillation amplitude and frequency of the double-tank autodyne oscillator as well as the auto-detecting phenomenon. These equations can be also used for calculation of the double-tank autodyne with supply circuit modulation by means of variation of  $E$  voltage, when  $a_0 = f_{mdl}(t)$  represents the modulating function.

It is necessary to note that although the equation system (18)–(20) has been obtained by means of linearization of the AE nonlinear conductances  $\bar{G}_e(E, A, \omega)$  and  $\bar{B}_e(E, A, \omega)$ , it is nonlinear since in the general case these equations cannot be solved with respect to variable  $\chi$  and, moreover, the phase variations  $\delta(t, \tau)$  can be large enough.

### Autodyne characteristics and their analysis

The further investigation on a base of the equation system (18)–(20) is carried out under certain

simplifying assumptions and without taking into account the oscillator modulation in the supply circuit supposing  $a_0 = 0$ . Then for each equation of the system (18)–(20) the first term will be eliminated since we can neglect the reaction of this circuit. At that, the auto-detecting response  $i_0$  for the AE current variation can be found out according to equation (20) at substitution in it the responses  $a_1$  and  $\chi$  obtained from the system (18), (19).

In contrast to resistive  $G_{os}$  and reactive  $B_{os}$  conductances, the value of  $Y_e$  is the slowly-varying function of frequency. Therefore, to simplify an analysis we can consider in (19) only parameters  $\xi_1$  and  $\xi_2$  since  $\xi_1 + \xi_2 = \xi_{12} \gg \xi_e$ .

To simplify further examination, we consider the linear case only, when due to the high  $Q$ -factor  $Q_{c2}$  and the relative small level of reflected radiation, the amplitude of autodyne frequency variations  $\chi$  is so small that we can neglect the influence of the non-linearity parameter  $\varepsilon_{n2}$ . Then the equation system (18), (19) takes the form:

$$\alpha_{11}a_1 + \varepsilon_1\chi = \Gamma(t, \tau)\eta\cos \delta(t, \tau); \quad (21)$$

$$\beta_{11}a_1 + \xi_{12}\chi = -\Gamma(t, \tau)\eta\sin \delta(t, \tau). \quad (22)$$

Having this system solved by the Kramer method, after some transformation we obtain equations for the instantaneous values of  $u_0(t) = u_0$ ,  $a_1(t) = a_1$  and  $\omega(t) = \chi(t)\omega_0$ :

$$u_0(t) = Z_0 i_0 = \Gamma(t, \tau)K_0 Z_0 \cos [\delta(t, \tau) - \psi_0]; \quad (23)$$

$$a_1(t) = \Gamma(t, \tau)K_a \cos [\delta(t, \tau) - \psi_1]; \quad (24)$$

$$\omega(t) = \omega_0 - \Gamma(t, \tau)\omega_0 L_{a2} \sin [\delta(t, \tau) + \theta], \quad (25)$$

where  $K_0 = (\alpha_{01}K_a \cos \psi_1 - \varepsilon_0 L_{a2} \sin \theta) / \cos \psi_0$  is the coefficient of autodyne response auto-detecting characterizing the process of its transition into the AE bias circuit;  $K_a = \eta \xi_{12} / \Delta \cos \psi_1$  is the coefficient of autodyne amplification showing how much the autodyne response on the amplitude variation is more than the amplitude of radiation returned from the reflecting object [12];  $L_{a2} = \eta \alpha_{11} / \Delta \cos \theta$  is the factor of autodyne frequency deviation;  $\psi_0 = \arctan[(\alpha_{01}K_a \sin \psi_1 - \varepsilon_0 L_{a2} \times \cos \theta) / (\alpha_{01}K_a \cos \psi_1 - \varepsilon_0 L_{a2} \sin \theta)]$ ,  $\psi_1 = \arctan(\varepsilon_1 / \xi_{12})$ ,  $\theta = \arctan(\gamma)$  are angles of the signal relative phase shift in the AE supply circuit, autodyne variations of amplitude and frequency, respectively;  $\gamma = \beta_{11} / \alpha_{11}$  is the coefficient of oscillator's anisochronous property;  $\Delta = \alpha_{11}\xi_{12} - \beta_{11}\varepsilon_1$  is the determinant of the system (21), (22);  $Z_0$  is the impedance of autodyne current variation conversion into the voltage by means of the registration unit [18].

Equations (23)–(25) have the same view as equations obtained for the usual single-tank autodyne [12]. Coefficients of auto-detecting  $K_0$  and autodyne amplification  $K_a$  incoming in these equations are similar for both cases. However, values of factors of autodyne frequency deviation of the usual  $L_{a1}$  and stabilized  $L_{a2}$  oscillators differ considerably. Taking into account an inequality  $\alpha_{11}\xi_{12} \gg \beta_{11}\varepsilon_1$ , which is true for most oscillators, we obtain the relation between values  $L_{a1}$  and  $L_{a2}$ , indicating the degree of decreasing of the autodyne frequency deviation:

$$S_f = \frac{L_{a1}}{L_{a2}} = \frac{Q_{equ}}{Q_{L1}} = 1 + \frac{Q_{c2}\beta_1\beta_2}{Q_{L1}(1 + \beta_2)^2}. \quad (26)$$

The value  $S_f$  represents the stabilization coefficient by analogy with the theory of usual oscillators, which indicates the effectiveness of the means for decrease of any disturbance influence [25].

Let us consider now a behavior of phase  $\delta(t, \tau)$  incoming into equations for the autodyne response (8), (9), (18), (19), (21)–(25), which is defined as  $\delta(t, \tau) = \Psi(t) - \Psi(t, \tau)$ . Having expanded functions  $\Gamma(t, \tau)$  and  $\Psi(t, \tau)$  into the Taylor series on the delay time of reflected radiation and limiting by two first expansion terms, we obtain the solution for the module  $\Gamma(t, \tau) = \Gamma$  and phase  $\delta(t, \tau) = \omega(t)\tau$ . Taking into account the equality (25) the last expression for phase can be written as:

$$\delta(t, \tau) = \omega_0 \tau - p_{a2} \sin [\delta(t, \tau) + \theta], \quad (27)$$

where  $p_{a2} = \Delta \omega_m \tau$  is the distortion parameter of the autodyne signal [12];  $\Delta \omega_m = \Gamma \omega_0 L_{a2}$  is the value of the autodyne frequency deviation, which is defined by the relative level of reflected radiation  $\Gamma$  and the inherent oscillator parameters.

The analysis of expressions obtained allows us to clarify a role of the distortion parameter  $p_{a2}$  in formation of the autodyne response. Consider the key characteristics of oscillator under condition of the uniform movement of the reflecting object. Suppose that the phase in equation (27) changes linearly and continuously with the speed  $2\pi$  rad/sec because of the specified movement of the object on the analyzing interval of normalized time  $\tau_d = \omega_0 \tau / 2\pi$ . Then according to theory of short-range radar systems we obtain the phase characteristic (PC) equation to define the phase shift of the reflected wave

$$\delta(\tau_d) = 2\pi\tau_d - p_{a2} \sin [\delta(\tau_d) + \theta]. \quad (28)$$

The equation (28) as well as (27) is transcendental one since its left and right parts contain insoluble vari-

able  $\delta(\tau_d)$ . To solve (28) we use the method of successive approximations [14]. According to this method, we successively substitute the approximate values of the phase  $\delta(\tau_d)$  into the right part of the equation (28). As a result we obtain the solution of (28) for the general case of  $n$ -th approximation. The obtained expression for the steady-state phase values can be written as follows:

$$\delta(\tau_d)_{(n)} = [2\pi\tau_d]_{(0)} - p_{a2}\sin\{[2\pi\tau_d]_{(1)} + \theta - p_{a2}\sin\{[2\pi\tau_d]_{(2)} + \theta - \dots p_{a2}\sin\{[2\pi\tau_d]_{(n)} + \theta\} \dots\}, \quad (29)$$

where indices in parenthesis designate the order of approximation.

Autodyne responses in the form of variations of the AE bias current  $u_0$  and oscillation amplitude  $a_1$  in equations (23), (24) differ by angles of the relative phase shifts  $\psi_0$  and  $\psi_1$  only. Therefore, further calculations will be carried out for the generalized response  $a(\tau_d)$  which denotes both values  $u_0(\tau_d)$  and  $a_1(\tau_d)$  taking into account the relative phase shift angle  $\psi$ .

Using (29) the steady-state values of the normalized characteristics of the autodyne frequency variations  $\chi_d(\tau_d)$  and the generalized response  $a_d(\tau_d)$  in  $n$ -th approximation can be expressed as:

$$\chi_d(\tau_d) = \chi(\tau_d)/\chi_m(\tau_d) = -\sin\{[2\pi\tau_d]_{(0)} + \theta - p_{a2}\sin\{[2\pi\tau_d]_{(1)} + \theta - p_{a2}\sin\{[2\pi\tau_d]_{(2)} + \theta - \dots - p_{a2}\sin\{[2\pi\tau_d]_{(n)} + \theta\} \dots\}, \quad (30)$$

$$a_d(\tau_d) = a(\tau_d)/a_m(\tau_d) = \cos\{[2\pi\tau_d]_{(0)} - \psi - p_{a2}\sin\{[2\pi\tau_d]_{(1)} + \theta - p_{a2}\sin\{[2\pi\tau_d]_{(2)} + \theta - \dots - p_{a2}\sin\{[2\pi\tau_d]_{(n)} + \theta\} \dots\}, \quad (31)$$

where  $\chi_m(\tau_d)$  and  $a_m(\tau_d)$  are the amplitude frequency variations and the generalized response. According to [11–14], we will designate the quantities  $\chi_d(\tau_d)$  and  $a_d(\tau_d)$  as a frequency characteristic of autodyne (FCA) and an amplitude characteristic of autodyne (ACA).

The normalized phase characteristics and their derivatives calculated according to (29) are represented in Fig. 4a and Fig. 4b where curves 1 are related to the case of the usual oscillator having  $p_{a1} = 0.8$  as well as curves 2 are concerned with the stabilized oscillator for which  $p_{a2} \ll 1$ . For these cases the normalized FCA  $\chi_d(\tau_d)$  and ACA  $a_d(\tau_d)$  calculated according to (30), (31) are depicted in Fig. 4c and Fig. 4d respectively, where the curves numeration is the same as in previous consideration.

The analysis of these characteristics indicates that the autodyne frequency variations of the non-stabilized oscillator cause irregularities of the phase shift of the

reflected wave as shown in Fig. 4a. At that, the variation speed of the phase shift characterized as the instantaneous frequency difference of radiated and reflected oscillations  $\Omega_a(\tau_d) = d[\delta(\tau_d)]/d\tau_d$  takes the oscillating character with formation of peaks of the instantaneous frequency as shown in Fig. 4b. A height of these instantaneous frequency peaks increases with the growth of the distortion parameter  $p_{a1}$ . As follows from Fig. 4b, these oscillations of instantaneous frequency  $\Omega_a(\tau_d)$  of the autodyne response are observed relative to its average value, which is equal to Doppler shift frequency  $\bar{\Omega}_a = \Omega_D$ .

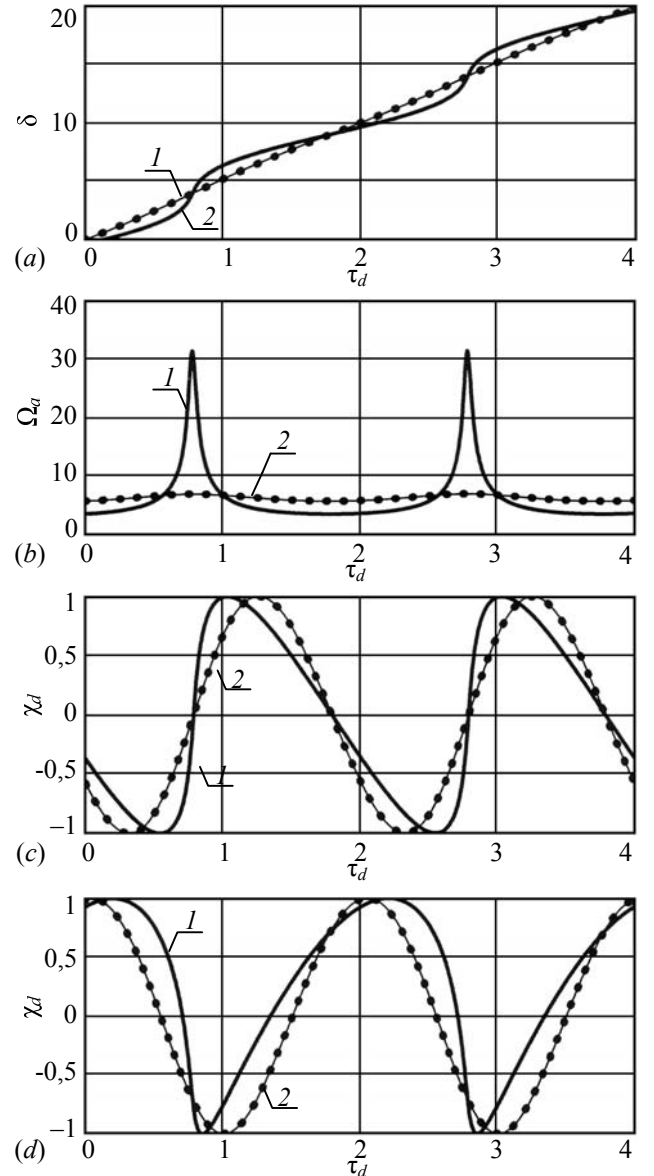


Fig. 4. Normalized phase characteristics (a), their derivatives (b), frequency (c) and amplitude (d) characteristics of autodyne oscillators calculated at  $\theta = 1$  and different values of distortion parameters: (1)  $p_{a1} = 0.8$ ; (2)  $p_{a2} \ll 1$ .



Irregularity of the phase shift of the reflected wave  $\delta(\tau_d)$  is a reason of ACA distortions and additional deformations of FCA as can be seen in Fig. 4c and Fig. 4d, at which the wave inclination effect is observed. Direction of this inclination depends on the value of coefficient of oscillator anisochronous property  $\gamma_1$ , the angle  $\psi$  characterizing a coupling type with a load (coupling more than critical or less that critical), and the relative direction of the reflecting object motion. The degree of inclined distortions increases with the growth of the parameter  $p_{a1}$ . At further increase of this parameter, when it exceeds unity, the waveform becomes qualitatively another. This change consists in the appearance of the wave front jumps instead of the sharp wave front.

It should be emphasized the principal differences of FCA and ACA distortions that are clearly visible from comparison of curves 1 and 2 in Fig. 4c and Fig. 4d. At the variation of parameter  $p_{a1}$  the half-waves of FCA remain always symmetrical with keeping the transition phase through zero. However, the areas of the positive and negative ACA half-waves are different, that indicates the presence of DC component in the autodyne response. The position of transition points through zero considerably depends on the value of parameter  $p_{a1}$ , defining the level of the reflected signal. When the parameter  $p_{a1}$  changes the observed offset of the gentle waveform front has the reverse direction with respect to the offset of the sharp front.

The behavior of curves 2 in Fig. 4 calculated for  $p_{a2} \ll 1$  shows that PC of the stabilized oscillator has a linear dependence versus the variable  $\tau_d$  as well as FCA and ACA vary practically according to a harmonic law. As follows from Fig. 4b, the instantaneous frequency difference  $\Omega_a$  of the autodyne response varies weakly and practically always equals to the frequency of the Doppler shift  $\Omega_a = \Omega_D$ , as in radar with homodyne structure of a transceiver.

For descriptive presentation of processes in the autodyne oscillator we will use the autodyne's amplitude-frequency characteristic (AFC). It represents the autodyne frequency variations as a function of amplitude variations and characterizes the biunique correspondence between FCA and ACA [13]. This characteristic usually has a form of an ellipse, which eccentricity and the axis slope angle depend on parameters of the oscillator under investigation. Therefore, in the general theory of oscillators such characteristic is called the ellipse of oscillator pulling by a load [28] and in this case it serves as a tool for research of autodyne inherent properties.

An example of the autodyne AFC calculated for the usual oscillator with offset angles  $\psi = 0$ ,  $\theta = 1$  and at  $p_{a1} = 0.8$  is presented in Fig. 5. The ellipse projections on its axes give the appropriate values of ACA and FCA depending on the value of  $\tau_d$ . Ellipse parameters and its orientation depend on the angle  $\theta$  and on the character of oscillator coupling with a load. The calculation origin on the ellipse, at which  $\delta(\tau_d) = 0 + n$ , where  $n$  is the turnover number, is marked by the bold point.

Positions of the image point through one tenth of the autodyne response period are designated by the circles. At growth of delay time  $\tau_d$  the image point moves along the ellipse counter clockwise. If the delay time decreases, the image point moves along the ellipse counter in the reverse direction. In general case its motion speed is non-uniform, which is clearly seen on intervals between circles. With the growth of the parameter  $p_{a1}$  this speed increases on the lower part of the ellipse and decreases at the upper part. The analysis of this motion speed can be used for determination of the movement direction of reflecting objects [10]. The image point motion becomes uniform in the case of the stabilized oscillator only, when  $p_{a2} \ll 1$ .

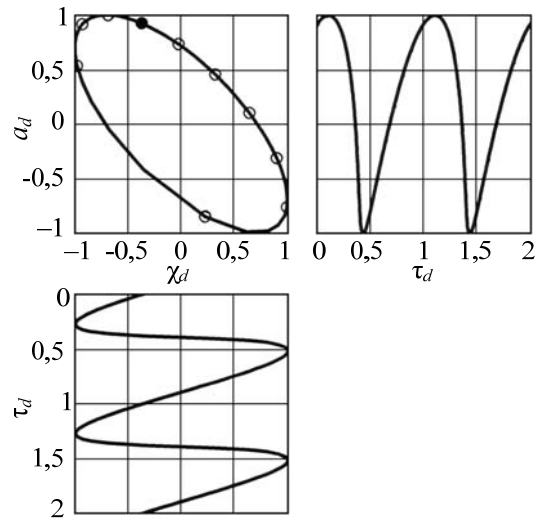


Fig. 5. The amplitude-frequency  $a_d(\chi_d)$ , the amplitude  $a_d(\tau_d)$  and frequency  $\chi_d(\tau_d)$  characteristics of the autodyne oscillator, calculated for  $\theta = 1$ ;  $p_{a1} = 0.8$ .

Results obtained in this section show that the stabilized autodyne oscillator provides essential reduction of the frequency deviation value and reduction of the distortion degree of signals at keeping of the functional possibilities of the autodyne systems as compared with the usual system. Effectiveness of considered method relative to stabilization of oscillating system frequency is high enough. For example, whereas the value of  $p_{a1}$



for the usual oscillator is closed to the critical value (nearly equal to unity), this parameter for the stabilized oscillator with the coefficient  $S_f = 30$  has the value  $p_{a2} \ll 1$ . This means that in considered case the autodyne signal is practically sinusoidal. However, in each specific case of any autodyne application in radar systems, it is expedient to calculate the distortion parameter taking into account the system functioning conditions.

### Calculation of the autodyne signal spectrum

The considered approach to solution of the transcendental equations (29)–(31) is suitable for the analysis of processes in the time domain. Another technique for solving these equations is based on the Bessel – Fubini expansions [14].

This technique is the most suitable procedure for calculation of the autodyne signal spectrum. According to this approach, one can obtain the following equations for the spectrum definition of the main components of the normalized autodyne response of the stabilized oscillator:

$$a_d(\tau_d) = a_1(\tau_d)/a_{1m} = A_0 + \sum_{n=1}^{\infty} A_n \cos[n(2\pi\tau_d) - n\psi - \varphi_n]; \quad (32)$$

$$\chi_d(\tau_d) = \Delta\omega_d(\tau_d)/\Delta\omega_m = \sum_{n=1}^{\infty} B_n \sin[n(2\pi\tau_d) + n\theta], \quad (33)$$

where  $A_0 = J_1(p_{a2})\cos\theta$  is the DC component and  $A_n = [(C_n \cos\theta)^2 + (B_n \sin\theta)^2]^{1/2}$  is the normalized amplitude of  $n$ -th harmonic of the generalized autodyne response;  $\varphi_n = \arctan[(B_n/C_n)\tan\theta]$  is the initial phase of  $n$ -th harmonic of the autodyne response;  $C_n = (-1)^{n-1}[J_{n-1}(np_{a2}) - J_{n+1}(np_{a2})]/n$  is the normalized amplitude of  $n$ -th harmonic of the autodyne response of the isochronous oscillator, which has the offset angle  $\theta = 0$ ;  $B_n = (-1)^n(2np_{a2})J_n(np_{a2})$  is the normalized amplitude of  $n$ -th harmonic of the autodyne frequency variations;  $J_n(np_{a2})$  is the Bessel function of the first kind.

The analysis of (32) and (33) shows that the position of gentle and sharp parts of autodyne amplitude variations of the non-isochronous oscillator is defined by initial phases  $\varphi_n$  of the higher harmonics of the autodyne response. Calculated spectral diagrams of FCA and ACA of the autodyne response for its normalized frequency  $F_d = 1/\tau_d$ , obtained according to (32), (33) for the usual oscillator at  $\theta = 1$  and  $p_{a1} = 0.8$ , are presented in Fig. 6.

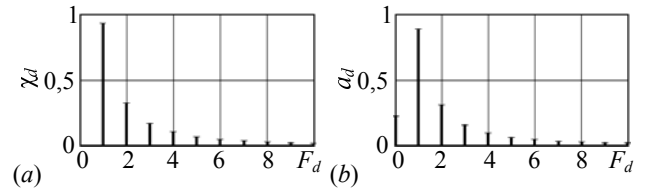


Fig. 6. Spectral diagrams of FCA (a) and ACA (b) of the autodyne response, calculated for  $\theta = 1$ ;  $p_{a1} = 0.8$ .

As follows from Fig. 6b, the autodyne response on the oscillation amplitude variation has DC component, the value of which is directly proportional to the Bessel function  $J_1(p_{a1})$ . The noticeable level of higher components at  $p_{a1} = 0.8$  can achieve the seventh harmonic. In contrast to the spectrum of amplitude variations  $a_d$  of the oscillator, in the spectrum of the frequency variation  $\chi_d$ , shown in Fig. 6a, the DC component is absent, that is  $B_0 = 0$ . It follows that the average value of the oscillator frequency remains invariable during an interaction of the oscillations with reflected radiation. Thus, under condition  $p_{a1} < 1$ , all frequency and phase relations for the autodyne signals remain invariable despite the presence of the distortions, and they completely correspond those for signals of homodyne systems [29]. This is quite an important result for the practical application of autodynes in the short-range radar systems.

Analysis of the stabilized autodyne with the same level of reflected radiation as usual oscillator shows that in the case when the parameter  $p_a \ll 1$  the signal from the point reflector is practically sinusoidal as well as the signals of the homodyne radar. As a result, we can obtain the solutions of equations (29)–(31) in the zero approximation supposing  $\delta(\tau_d)_{(n)} = [2\pi\tau_d]_{(0)}$ .

Developed analytical techniques for the time and spectral analysis of autodyne signals based on the methods of successive approximations and the Bessel – Fubini expansions are applicable if the distortion parameter  $p_{a1} < 1$  [14]. If the parameter  $p_{a1}$  approaches the unity, the number of terms to obtain the correct solution of (29)–(31) and the number of the Bessel – Fubini expansion terms in formulas (32), (33) increases significantly. For instance, if  $p_{a1} = 0.8$ , the satisfactory accuracy of the result can be obtained at  $n \geq 20$ .

### Non-linearity analysis on amplitude of the stabilized oscillator

If the reflected radiation level increases the value, when it is necessary to take into consideration the parameter of non-linearity on amplitude  $\varepsilon_{n2}$ , the section of frequency variations remains still linear enough as

shown in Fig. 3a and Fig. 3b. Therefore, the solution of the quasi-linear equation (25) can be carried out together with the equation (24), having the quadratic dependence on  $\chi$ . Supposing for simplicity of analysis that the oscillator is isochronous, when  $\beta_{11} = 0$ , we get:

$$a_1 = \Gamma(t, \tau) K_{a1} \{ -\Gamma(t, \tau) k_{a2} + \cos [\delta(t, \tau) - \psi_1] + \Gamma(t, \tau) k_{a2} \cos 2\delta(t, \tau) \}, \quad (34)$$

where  $K_{a1} = \eta_1 / \alpha_{11} \cos \psi_1$  is a coefficient of autodyne amplification of the isochronous oscillator, for which  $\beta_{11} = 0$ ;  $k_{a2} = \eta_1 \varepsilon_{n2} \cos \psi_1 / 2 \xi_{12}^2$  is an amplification coefficient of conversion products of the second order.

As follows from equation (34) the non-linear conversions of the autodyne response on amplitude variations lead to the appearance of the DC component and a harmonic with doubled value of the phase  $2\delta(t, \tau)$ . The level of these components is defined by the product of coefficients  $\Gamma(t, \tau)$  and  $k_{a2}$ .

Carrying out the normalization of the equation (34) relative to response amplitude  $\Gamma(t, \tau) K_{a1}$ , we obtain:

$$a_1 = -a_{m2d} + \cos [\delta(t, \tau) - \psi_1] + a_{m2d} \cos 2\delta(t, \tau), \quad (35)$$

where  $a_{m2d} = \Gamma(t, \tau) k_{a2}$  is the relative level of the second harmonic. The solution of this equation in  $n$ -th approximation has a form:

$$a_{d12}(\tau_d) = \cos \{ [2\pi\tau_d]_{(0)} - \psi - p_{a2} \sin \{ [2\pi\tau_d]_{(1)} + \theta - p_{a2} \sin \{ [2\pi\tau_d]_{(2)} + \theta - \dots - p_{a2} \sin \{ [2\pi\tau_d]_{(n)} + \theta \} \dots \} \} - a_{m2d} + a_{m2d} \cos \{ [4\pi\tau_d]_{(0)} - p_{a2} \sin \{ [4\pi\tau_d]_{(1)} + \theta - p_{a2} \sin \{ [4\pi\tau_d]_{(2)} + \theta - \dots - p_{a2} \sin \{ [4\pi\tau_d]_{(n)} + \theta \} \dots \} \} \quad (36)$$

The results calculated according to (36) at values of the relative level of the second harmonic  $a_{m2d} = 0.2$  as well as at  $p_{a2} = 0.1$  and  $p_{a2} = 0.5$  are presented in Fig. 7b and Fig. 7d in the form of time and spectral diagrams of the autodyne response on amplitude variations. The similar diagrams calculated without taking into account the amplitude non-linearity are depicted in Fig. 7a and Fig. 7c for comparison. Fig. 8 illustrates the amplitude-frequency characteristics of the autodyne calculated at the same initial data as for features shown in Fig. 7.

Despite the high frequency stability of the oscillations and a small value of the distortion parameter  $p_{a2}$ , the additional signal distortions can occur in the autodyne at influence of reflected radiation of the high level as can be seen in Fig. 7b.

Under certain conditions the DC component in the autodyne response appearing due to the non-linearity on amplitude can compensate the DC component caused by PC non-linearity, as shown in Fig. 4a.

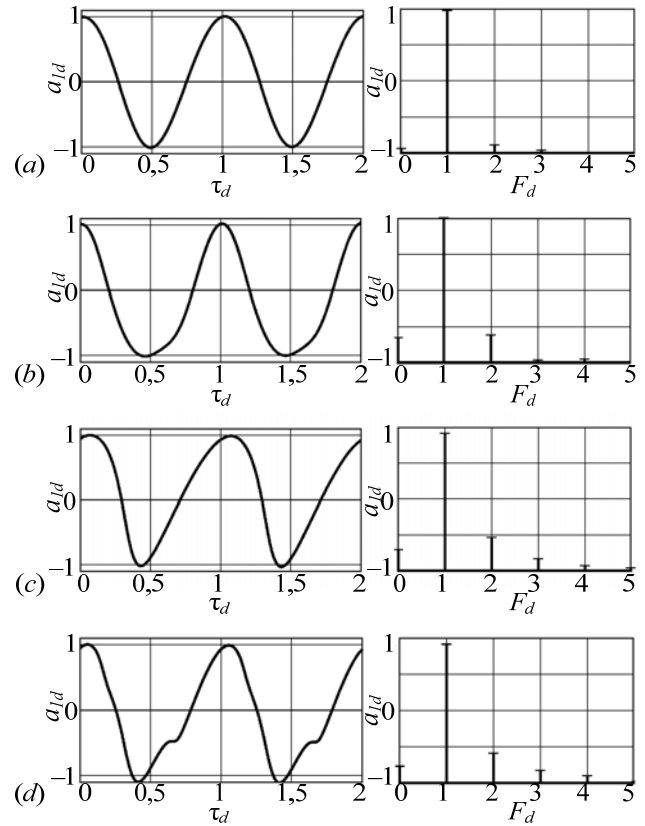


Fig. 7. Normalized time (left) and spectral (right) diagrams of autodyne signals of the stabilized oscillator calculated without taking into account (a), (c) and with the account (b), (d) of non-linearity on amplitude for  $\theta = 1, \psi_1 = 0, k_{a2} = 0.2$  and for different values of the distortion parameter: (a), (b)  $p_{a2} = 0.1$ ; (c), (d)  $p_{a2} = 0.5$ .

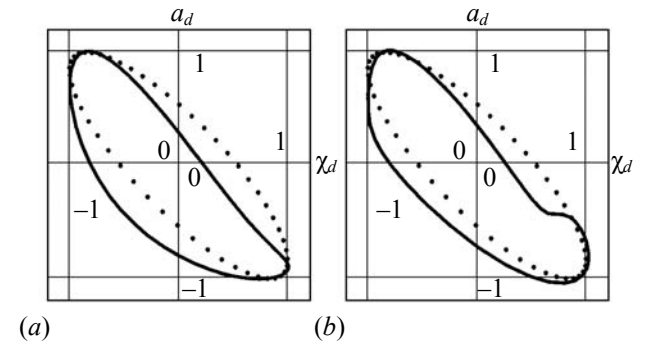


Fig. 8. Amplitude-frequency characteristics  $a_d(\chi_d)$ , calculated with taking into account of non-linearity on amplitude for  $\theta = 1, \psi = 1, k_2 = 0.2$  and for different values of the distortion parameter: (a)  $p_{a2} = 0.1$ ; (b)  $p_{a2} = 0.5$ . Curves presented by points are obtained at  $k_2 = 0$ .

The curves of Fig. 8 show that at appearance of the non-linearity on amplitude, the AFC form of the stabilized autodyne oscillator differs from the ellipsoid form typical for the usual single-tank autodynes. This indi-

cates the fact that a nature of given distortions is not linked with the irregularity of the phase shift of the reflected wave.

### Some aspects of stabilized autodyne application

Above-considered peculiarities of characteristic formation and respectively the output signals of the autodynes, which reveal the reasons of its distortions at increasing the reflected radiation level, have the great practical significance for correct application of the stabilized autodynes in short-range radar systems, both at the choice of oscillator parameters and at signal processing. The principle of frequency-phase measurements of signal parameters is the basis of algorithms of many processing methods. For implementation of this principle, time samples are provided in moments of signal transition through zero level, which ensures the minimal amplitude dependence of measurement results. However, positions of these points, as shown by curves  $I$  in Fig. 4d, considerably depend on the distortion parameter  $p_{d1}$  for signals registered on the basis of amplitude variation or the bias voltage variation in non-stabilized autodyne.

Moreover, variations of the reflected radiation level cause variations of DC component of the autodyne output signal. Although this component does not usually pass in the processing unit, the fast fluctuations of signal level may cause additional displacements of transition positions and, respectively, fluctuations of output signal fronts of the threshold device. Stabilized autodynes provide the essentially better signal quality and independence of transitions through zero upon the level of reflected radiation.

Application of frequency stabilization for the autodyne signal quality increase is necessary not only for the CW mode of non-modulated radiation but for systems with various types of modulation.

### Conclusion

The investigations of the autodyne signal features in the stabilized oscillators with the external high- $Q$  cavity are performed. It is proved that the main parameters of these oscillators including coefficients of auto-detecting and autodyne amplification are the same as in the non-stabilized oscillators. They also have the signal distortions as usual autodynes but their level is considerably lower due to the less value of the autodyne frequency deviation.

It is proposed to characterize the degree of frequency deviation reduction of the stabilized oscillator by the stabilization coefficient, which indicates how much the value of frequency deviation in the oscillator

under investigation is lower than in the usual oscillator for the same level of reflected radiation. The nonlinear distortions of the autodyne signal are revealed, which can be observed with growth of the reflected radiation level. In contrast to the single-frequency autodynes these distortions are caused not by autodyne frequency variations but by frequency dispersion of the oscillating system conductivity.

The results of investigations concerning the nature of these nonlinear distortions of the autodyne signal show that at autodyne frequency variations the additional amplitude modulation occurs on each edge of the frequency characteristic with doubled frequency. This modulation is superimposed the natural autodyne amplitude variations caused by the phase variation of the reflected wave.

The obtained results convincingly show the effectiveness of the external high-quality cavity application to improve technical indices of the autodyne short-range radar systems. For instance, the use of the stabilized autodynes allows us to decrease the signal distortions, to improve the spectrum of oscillator radiation, and to widen the dynamic range.

In further theoretical investigations of the stabilized autodynes it is necessary to take into account the non-linearity of the phase characteristic of the oscillating system as well as to examine the influence of the relative frequency detuning of cavities on the formation of the autodyne response.

The experimental investigations of stabilized autodynes are also interesting to make recommendations about their practical application in short-range radar systems.

The features of signals of the autodyne oscillator, which use various types of modulation and various ways of coupling of the basic and stabilizing cavities, also seem to be interesting and require further examination.

The authors would like to thank Petro Ya. Stepanenko for the serious study of paper materials and useful advices for their improvement.

### References

1. Page C. H., Astin A. V. Survey of proximity fuze development // American Journal of Physics. — 1947. — Vol. 15, N. 2. — P. 95—110.
2. Use of microstrip impedance — Measurement technique in the design of a BARITT diplex Doppler sensor / B. M. Armstrong, R. Brown, F. Rix, J. A. C. Stewart // IEEE Transaction on Microwave Theory and Techniques. — 1980. — Vol. 28, N. 12. — P. 1437—1442.
3. Yasuda A., Kuwashima S., Kanai Y. A shipborne-type wave-height meter for oceangoing vessels, using microwave

- Doppler radar // *IEEE Journal of Oceanic Engineering*. — 1985. — Vol. 10, N. 2. — P. 138–143.
4. Komarov I. V., Smolskiy S. M. *Fundamentals of short-range FM radar*. — Norwood: Artech House, 2003. — 289 p.
5. Zakarlyuk N. M., Noskov V. Ya., Smolskiy S. M. On-board autodyne velocity sensors for aeroballistics inspections // *Proceedings of 20th International Crimean Conference “Microwave & Telecommunication Technology”*, September 13–17, 2010. — Sevastopol: Weber. — 2010. — Vol. 2. — P. 1065–1068.
6. Noskov V. Ya., Smolskiy S. M. Main features of double-diode autodynes and its application // *Proceedings of 20th International Crimean Conference “Microwave & Telecommunication Technology”*, September 13–17, 2010. — Sevastopol: Weber. — 2010. — Vol. 2. — P. 1051–1054.
7. Usanov D. A., Scripal Al. V., Scripal An. V. *Physics of semiconductor RF and optical autodynes*. — Saratov: Saratov University Publisher, 2003. — 312 p. [in Russian].
8. Votoropin S. D., Noskov V. Ya. *Transceiver modules on the low-current Gunn diodes for autodyne systems // Electronic Techniques. Series 1. UHF techniques*. — 1993. — N. 4. — P. 70–72 [in Russian].
9. Votoropin S. D., Noskov V. Ya., Smolskiy S. M. Modern hybrid-integrated autodyne oscillators of microwave and millimeter ranges and their application. Part 1. Technological achievements // *Successes of modern electronic engineering*. — 2006. — N. 12. — P. 3–30 [in Russian].
10. New direction-of-motion Doppler detector / M. J. Lazarus, F. P. Pantoja, M. Somekh, et al // *Electronics Letters*. — 1980. — Vol. 16, N. 25. — P. 953–954.
11. General characteristics and peculiarities of the autodyne effect in oscillators / E. M. Gershenson, B. N. Tumanov, V. T. Buzykin, et al // *Radio Engineering and Electronics*. — 1982. — Vol. 27, N. 1. — P. 104–112 [in Russian].
12. Votoropin S. D., Noskov V. Ya., Smolskiy S. M. Modern hybrid-integrated autodyne oscillators of microwave and millimeter ranges and their application. Part 2. Theoretical and experimental investigations // *Successes of modern electronic engineering*. — 2007. — N. 7. — P. 3–33 [in Russian].
13. Votoropin S. D., Zakarlyuk N. M., Noskov V. Ya., Smolskiy S. M. On principal impossibility of autosynchronization of an autodyne by radiation reflected from a moving target // *Russian Physics Journal*. — 2007. — Vol. 50, N. 9. — P. 905–912.
14. Votoropin S. D., Noskov V. Ya., Smolskiy S. M. Modern hybrid-integrated autodyne oscillators of microwave and millimeter ranges and their application. Part 3. Functional features of autodynes // *Successes of modern electronic engineering*. — 2007. — N. 11. — P. 25–49 [in Russian].
15. Gershenson E. M., Putilov P. A. Investigation of three-cavities autodyne UHF system // *Radio Engineering and Electronics*. — 1969. — Vol. 14, N. 1. — P. 137–145 [in Russian].
16. Noskov V. Ya. Analysis of an autodyne UHF transducer for noncontact measurement and control of the dimensions of components // *Measurement Techniques*. — New York: Springer. — 1992. — Vol. 35, N. 3. — P. 297–301.
17. Votoropin S. D., Noskov V. Ya., Smolskiy S. M. Modern hybrid-integrated autodyne oscillators of microwave and millimeter ranges and their application. Part 4. Investigations of multi-frequency autodynes // *Successes of modern electronic engineering*. — 2008. — N. 5. — P. 65–88 [in Russian].
18. Noskov V. Ya., Smolskiy S. M. Autodyne signal registration in a power circuit of the semiconductor diode oscillator in microwave and millimeter ranges (Review) // *Techniques and Devices of the Microwave*. — 2009. — N. 1. — P. 14–26 [in Russian].
19. Kurokawa K. *An introduction to the theory of microwave circuits* // Academic Press, 1969. — 434 p.
20. Takayama Y. Doppler signal detection with negative resistance diode oscillators // *IEEE Transaction on Microwave Theory and Techniques*. — 1973. — Vol. 21, N. 2. — P. 89–94.
21. Votoropin S. D., Noskov V. Ya., Smolskiy S. M. An analysis of the autodyne effect of oscillators with linear frequency modulation // *Russian Physics Journal*. — 2008. — Vol. 51, N. 6. — P. 610–618.
22. Votoropin S. D., Noskov V. Ya., Smolskiy S. M. An analysis of the autodyne effect of a radio-pulse oscillator with frequency modulation // *Russian Physics Journal*. — 2008. — Vol. 51, N. 7. — P. 750–759.
23. Votoropin S. D., Noskov V. Ya., Smolskiy S. M. Modern hybrid-integrated autodyne oscillators of microwave and millimeter ranges and their application. Part 5. Investigations of frequency-modulated autodynes // *Successes of modern electronic engineering*. — 2009. — N. 3. — P. 3–50 [in Russian].
24. Noskov V. Ya., Smolskiy S. M. Modern hybrid-integrated autodyne oscillators of microwave and millimeter range and their applications. Part 6. Research of radio-pulse autodynes // *Successes of modern electronic engineering*. — 2009. — N. 6. — P. 3–51 [in Russian].
25. Shelton E. J. Stabilization of microwave oscillations // *IRE Transactions*. — 1954. — Vol. ED 1, N. 4. — P. 30–40.
26. Kohiyama K., Momma K. A new type of frequency-stabilized Gunn oscillator // *Proceedings of the IEEE*. — 1971. — Vol. 24, N. 10. — P. 1532–1533.
27. Stroganova E. P., Ivanov E. N., Tsarapkin D. P. UHF oscillator of combined frequencies // *Izvestiya Vysshikh Uchebnykh Zavedeniy. Radioelektronika*. — 1981. — Vol. 24, N. 10. — P. 69–72 [in Russian].
28. Malyshev V.A., Razdobudko V.V. Application of frequency and power pulling for the UHF oscillator by an external load to measure nonlinear parameters of its electronic conductivity // *Izvestiya Vysshikh Uchebnykh Zavedeniy. Radioelektronika*. — 1977. — Vol. 20, N. 1. — P. 45–51 [in Russian].
29. Skolnik M. I. *Introduction to radar systems*. — McGraw-Hill Book Company, 1962. — 748 p.